Two-Transmitter Wireless Power Transfer with LCL Circuit for Continuous Power in Dynamic Charging

***Abstract*—Wireless power transfer is a safe and convenient method for charging electric vehicles (EV). Dynamic charge can further reduce the needs of high capacity, heavy and costly batteries. Long transmitter coils provide steady power flow for certain distance. However coupling between the long coils with small coils is prone to field leakage and lower efficiency. Therefore, simultaneous two-transmitter method is proposed to emulate the long transmitter coils. LCL configuration is used for each transmitter to allows inverter sharing.**

***Keywords*—Wiress Power Transfer, LCL, Dynamic Charging, Neumann formula, Two-Transmitter**

I. Introduction

Electric vehicles are cleaner, quieter and more efficient compared to internal combustion engine. More importantly, the energy can be generated from renewable sources such as solar power and wind power. Dynamic charge [1]-[6] has been researched recently to solve the long charging time and further increase the appeal of EVs to general users [1]. Existing dynamic system [2], [3], [4] have long transmitter tracks that are well suited for large vehicles. Other example of long track system proposed by [5] has small vertical air-gap. When coupling long coil with small receiver, the efficiency is lower. This phenonema is explained using Neumann formula and maximum efficiency formula. Additionally, leakage maybe higher as the smaller receiver cannot capture the field [7], [8] .

Since long coils for dynamic charge results in low efficiency, [6] used small transmitter (ground pad) and pulsed power when the vehicle is detected. In this paper, a method to provide continuous power and high efficiency is proposed. With continuous power, constant current charging which is the desirable charging method for battery and EDLC [9] can be implemented. Small transmitters are arranged along the ground, two transmitters are activated at a time when the EV passby. Impedance inverter LCL circuit is used [6], [10] to ensure constant current in the activated transmitters. When the vehicle moves away, the no-load condition will cause zero reflected impedance from the receiver circuit to the primary circuit [11], [12]. Having constant current in the transmitters will not short circuit the inverter as in the primary series-compensated configuration and therefore multiple transmitters can be connected in parallel to an inverter. Futhermore, the compensation does not depend on the changes of the load and mutual inductance as in the primary parallel-compensated configuration [12]. Efficiency analysis and optimised load is also proposed for the two-transmitter system. Experiments were performed to verify the proposed method.

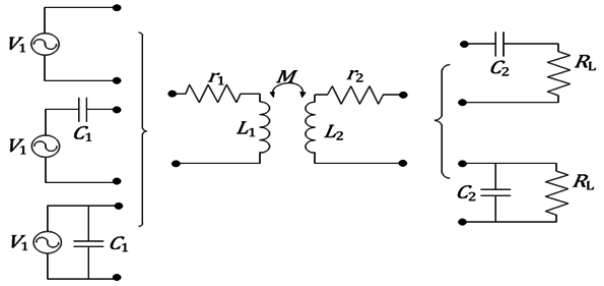

Figure 1. Compensation methods of wireless power transfer.

II. Long Coil Consideration

A. Maximum Efficiency

The equivalent circuits of six basic compensation methods are shown in Fig. 1. They are the series-series, series-parallel, parallel-series, parallel-parallel, uncompensated primary-series and uncompensated primary-parallel. The maximum efficiency of all six configurations is given in (1) [13].

$$\eta_{\max} = \frac{X}{(1+\sqrt{1+X})^2} \tag{1}$$

where

$$X = k^2 Q_1 Q_2 = \frac{(\omega_0 M)^2}{r_1 r_2} \tag{2}$$

and k is the coupling coefficient, Q_1 and Q_2 are the quality factors of transmitter and receiver respectively.

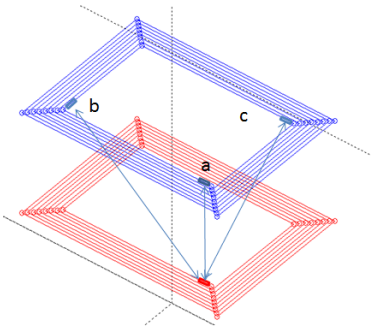

Figure 2. Neumann formula calculation method.

Figure 3. Fabricated 3 meter coil and receiver coil

Equation (1) tells us that the maximum efficiency will be close to 1 if X is much larger than 1. Mutual inductance, M is calculated using Neumann formula which will be explained in the next subsection. Coil resistance r_1 and r_2 are obtained from real measurements.

B. Neumann Formula

Mutual inductance between two coupled coils is given in (3) where the coils are divided into small sections shown in Fig. 2.

$$M = \frac{\mu_0}{4\pi} \oint_{C_1} \oint_{C_2} \frac{dl_1.dl_2}{D} \tag{3}$$

dl_1 and dl_2 are the differential length of these small sections of transmitter and receiver respectively. Term D is the distance between the sections. Mutual inductance is sum of mutual inductance contributed by each of these small sections.

For mounting at the EV Toyota Coms in the laboratory, a 10 turn receiver, outer size (40x40) cm receiver is

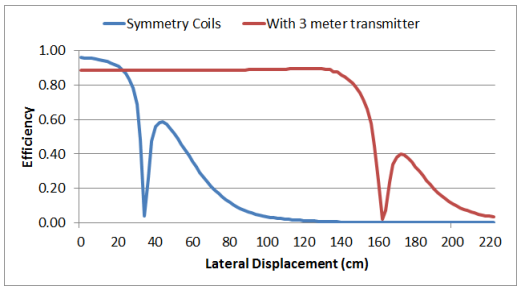

Figure 4. Plot of maximum efficiency vs lateral displacement.

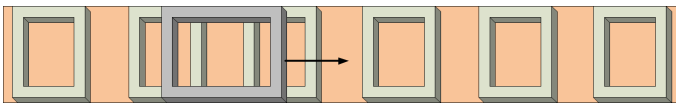

Figure 5. Illustration of the proposed method.

chosen. Transmitter length is extended to achieve larger charging coverage. The overlapping area of the coils is similar with using identical transmitter and receiver case. The resulted mutual inductance is similar, however with a longer transmitter, the coil resistance is larger. From Neumann calculations, when using identical coils and with 10 cm vertical gap, the mutual inductance is 22.98 μH and the coil resistance is measured to be 0.26 Ω. Therefore using (1) and (2), the maximum efficiency is 95.9%. A 10 turn, (40x300) cm transmitter shown in Fig. 2 is fabricated and the coil resistance is measured to be 1.52 Ω. The mutual inductance calculated using Neumann formula when placing the (40x40) cm receiver 10 cm above the middle of long transmitter is 19.41 μH and the maximum efficiency is reduced to 88.6%. Fig. 4 shows the efficiency plot vs lateral displacement of the receiver when the vertical gap is 10 cm. The 0 cm point is refer to the center of transmitter. If longer transmitter is used, the maximum efficiency will tend to reduce further.

III. Two Transmitters to One Receiver with LCL

Since coupling a long transmitter with small receiver results in low efficiency and may cause field leakage to the environment, simultaneous charging from two small transmitters is proposed. The receiver coil is made longer than the transmitter coils. Fig. 5 shows an illustration of the proposed method where the transmitter coils are arranged along the ground. When the receiver is above the first and second transmitter, these two transmitters are activated. When the receiver is moving towards the third transmitter, the second and third transmitter are activated and so on. LCL circuit is used for each transmitter to

978-1-4799-6610-3/15/$31.00 ©2015 IEEE

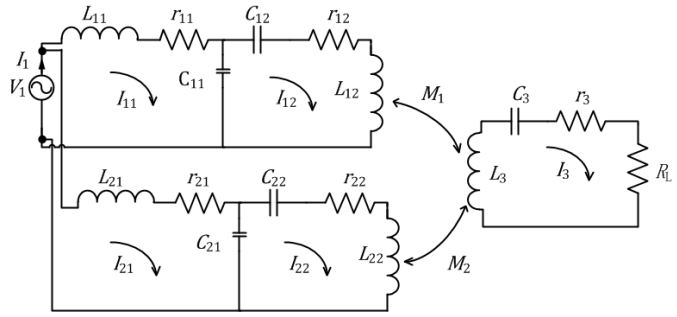

Figure 6. Equivalent circuit of the proposed method.

allow multiple small transmitters to be connected in parallel to a common inverter. Constant current is achieved at the transmitters and the low coupling condition or no-load condition will not short circuit the inverter.

Fig. 6 shows the equivalent circuit of the proposed wireless power trasnfer system. The components at the primary side are designed such that:

$$\begin{aligned} \omega_0 L_{11} &= \frac{1}{\omega_0 C_{11}} = \omega_0 L_{12} - \frac{1}{\omega_0 C_{12}} \\ \omega_0 L_{21} &= \frac{1}{\omega_0 C_{21}} = \omega_0 L_{22} - \frac{1}{\omega_0 C_{22}} \\ Z_{11} &= r_{11} + j(\omega_0 L_{11} - \frac{1}{\omega_0 C_{11}}) \approx 0 \\ Z_{21} &= r_{21} + j(\omega_0 L_{21} - \frac{1}{\omega_0 C_{21}}) \approx 0 \end{aligned} \quad (4)$$

Resistor r_{11} and r_{21} are the parasitic resistance of the inductor $L_{11}$and L_{21} respectively and is assumed to be sufficiently small. Looking at the I_{11} and I_{12} current loop:

$$\begin{aligned} V_1 &= Z_{11} I_{11} + \frac{-j}{\omega_0 C_{11}} I_{12} \\ V_1 &= Z_{21} I_{11} + \frac{-j}{\omega_0 C_{21}} I_{22} \end{aligned} \quad (5)$$

Since impedance Z_{11} and Z_{21} are zero, transmitter current I_{12} and I_{22} are constant. Furthermore applying the same design in every parallel branch and from the I_3 current loop:

$$\begin{aligned} I_{12} &= I_{22} \\ 0 &= I_3(R_L + r_3) + j\omega_0 M_1 I_{12} + j\omega_0 M_2 I_{22} \\ I_3 &= -\frac{j\omega_0(M_1 + M_2)}{(R_L + r_3)} I_{12} \end{aligned} \quad (6)$$

where secondary resonance is implemented:

$$j(\omega_0 L_3 - \frac{1}{\omega_0 C_3}) = 0 \quad (7)$$

Since the transmitter current is constant, receiver current I_3 will be constant if we can ensure the sum $(M_1 + M_2)$ is constant. Thus power received by the load will also be constant.

A. *Efficiency Analysis*

The transfer efficiency is given in (8).

$$\eta = \eta_{\text{pri}} \times \eta_{\text{sec}} \quad (8)$$

where

$$\eta_{\text{sec}} = \frac{R_L}{R_L + r_3} \quad (9)$$

and

$$\eta_{\text{pri}} = \frac{|I_3|^2(R_L + r_3)}{|I_3|^2(R_L + r_3) + |I_{12}|^2(r_{12}) + |I_{22}|^2(r_{22})} \quad (10)$$

Substituting (6) into (10) and cancelling the common terms, we obtain:

$$\eta_{\text{pri}} = \frac{\frac{(\omega_0 M_1 + \omega_0 M_2)^2}{(R_L + r_3)}}{\frac{(\omega_0 M_1 + \omega_0 M_2)^2}{(R_L + r_3)} + r_{12} + r_{22}} \quad (11)$$

Equation (8), (9) and (11) have the same structure as the series-series wireless power transfer. Therefore the same maximum efficiency equation with modification can be used. In this two transmitter case, the maximum efficiency is the same as (1). However the X is now given as:

$$X = \frac{(\omega_0 M_1 + \omega_0 M_2)^2}{(r_{12} + r_{22}) r_3} \quad (12)$$

and the load for maximum efficiency is:

$$R_{\text{Lmax}} = \sqrt{r_3 \left[\frac{(\omega_0 M_1 + \omega_0 M_2)^2}{r_{12} + r_{22}} + r_3 \right]} \quad (13)$$

Equation (13) is modified version of the maximum efficiency load equation from [14].

978-1-4799-6610-3/15/$31.00 ©2015 IEEE

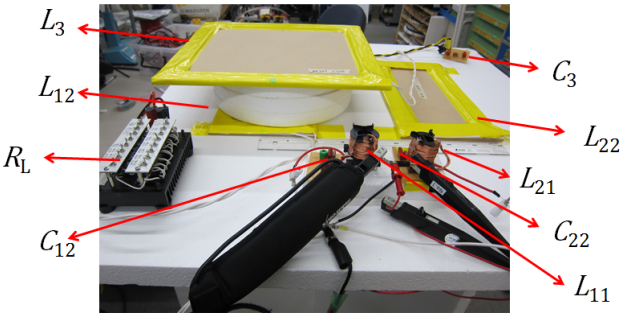

Figure 7. Experiment setup.

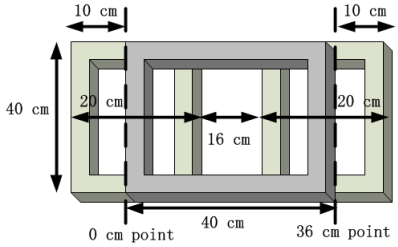

Figure 8. Coil Dimension

Table I
PARAMETER LIST

Parameter	Value
V_1	30 V
L_{11}	30 μH
r_{11}	0.1 Ω
C_{11}	110 nF
L_{12}	55.3 μH
r_{12}	0.25 Ω
C_{12}	136 nF
L_{21}	30 μH
r_{21}	0.1 Ω

Parameter	Value
C_{21}	110 nF
L_{22}	56 μH
r_{22}	0.26 Ω
C_{22}	136 nF
L_3	88.9 μH
r_3	0.33 Ω
C_3	38.5 nF
R_L	5 Ω

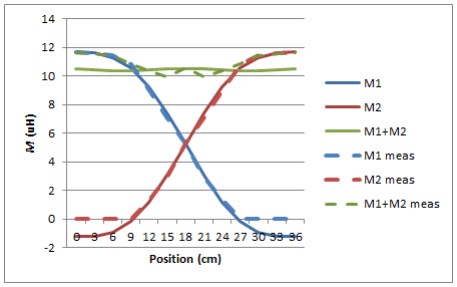

Figure 9. Mutual inductance plot.

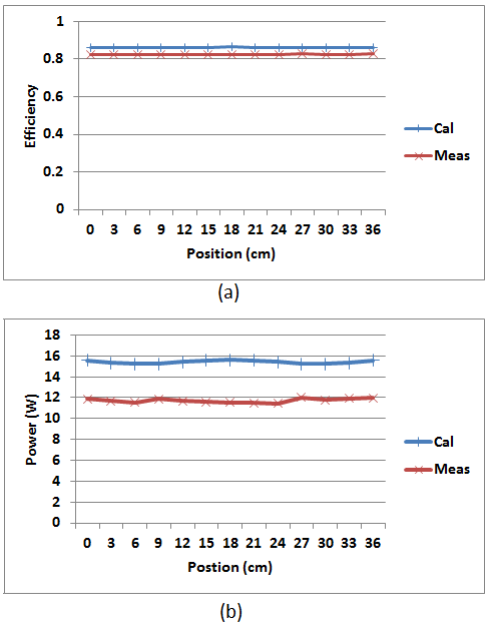

Figure 10. (a) Transfer Efficiency and (b) power for 0 cm point to 36 cm point.

B. Experiment

Fig. 7 shows the coils used for the experiment to verify the proposed method. The dimensions are shown in Fig. 8 and the component parameters are listed in Table III. The horizontal gap bewteen two transmitters is chosen such that sum the (M_1+M_2) is constant where M_1 is the mutual inductance between receiver and left transmitter and M_2 is the mutual inductance between the receiver and the right transmitter. Both the transmitters are identical and the vertical gap is 10 cm. Plot in Fig. 9 shows the mutual inductance plots where the horizontal axis is the position of the center of the receiver and the 0 cm point and 36 cm point are indicated in Fig. 8. The solid lines are the calculation data using Neumann Formula implemented in Matlab. The dotted lines are the measurement data using open-short method with a LCR meter. As shown by the plots, the measurement data matches with the calculation data except for the negative mutual inductance region where the open-short method is not valid.

The power supply used is NF HSA4014 high speed bipolar amplifier and the 85 kHz squarewave input reference is provided by Tektronix AFG3021 arbitrary/function generator. The voltage and current waveforms are captured using Tektonix MSO3034 mixed signal oscilloscope. Power and efficiency measurements are performed using NFL PPA5530 precision power

978-1-4799-6610-3/15/$31.00 ©2015 IEEE

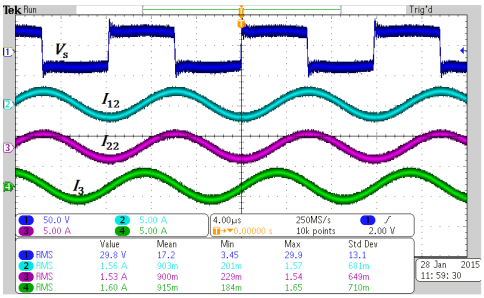

Figure 11. Voltage and current waveforms a) Source voltage and current at the coils, source current, I_s, I_{11} and I_{21} at b) 0 cm, c)18 cm and d) 36 cm

analysers. Efficiency plots in Fig. 10(a) shows that the efficiency maintain constant when the center of the receiver travels from 0 cm point to 36 cm point. The measurement data is close enough to calculation data. R_L is chosen to be the optimised load 5 Ω. The power plots is shown in Fig. 10(b), the power across R_L remains constant throughout the experiment region. The lower measured power is due to the reactive impedance seen by the power source that is not accounted by the derived equations above. The imaginary impedance is caused by the imperfect matching and harmonics that is present at the power source. Compared to SS configuration, where the resonant circuit is connected directly to the source, these harmonics from squarewave voltage output is not filtered at the source.

The voltage source waveform, current waveforms of the transmitters, current I_{12} and current I_{22}, and receiver I_3 are shown in Fig. 11. These waveforms remain nearly unchanged throughout the lateral displacement experiment therefore only one of them is shown. The amplitude of the squarewave is 30 V and taking only the fundamental components and according to (5) the RMS transmitter current are:

$$I_{12} = I_{22} = \frac{4}{\sqrt{2} \times \pi} \times jV_1\omega_0 C_{11} = j1.69 \text{ A} \qquad (14)$$

and according to (6), the calculated RMS receiver current is

$$I_3 = 1.77 \text{ A} \qquad (15)$$

where $M_1 + M_2$ is taken to be in average of 10.44 μH. The measurements show the actual results are slightly lower than calculations.

IV. Conclusion

When coupling long coils with small coils of general size EVs, transfer efficiency tend to be lower. This phenomena is explained using Neumann formula. Additionally, leakage field may occur as most part of the activated transmitter is not covered by the receiver. However long coils are able to provide steady power flow for certain distance. Therefore, simultaneous charged by two short transmitters is proposed to emulate the long coils. LCL circuit is used in each transmitter to allow inverter sharing. The coil arrangement is designed such that, the sum of mutual inductance between the receiver and first transmitter and mutual inductance between the receiver and second transmitter is constant. In this way, receiver is able to receiver almost constant power while moving along the dynamic charging lane. The proposed method is verified by experiments.

Future work for this paper is to account for imperfect matching and imaginary impedance viewed by the inverter due to harmonics in the derived equations. Secondly, a DC/DC converter will be implemented at the receiver for charging voltage load such as batteries and supercapacitors and power control if the vehicle goes slightly off track.

References

[1] S. Chopra and P. Bauer, " Driving range extension of EV with on-road contactless power transfer—a case study," *IEEE Trans. Ind. Electron.*, vol. 60, no. 1, pp 329-338, 2013.

[2] J. Shin et al., "Design and implementation of shaped magnetic resonance based wireless power transfer system for roadway-powered moving electric vehicles," *IEEE Trans. Ind. Electron.,* Vol. 61, No 3. pp. 1179-1192, 2013.

[3] S. Ahn, N. P. Suh and D-H. Cho, " Charging up the road," *IEEE Spectrum*, vol. 50, no. 4, pp 48-54, 2013.

[4] J. Meins and S. Carsten, "Transferring energy to a vehicle," WO Patent 000 494 Jan. 7, 2010.

[5] M. L. G. Kissin, G. A. Covic and J. T. Boys, "Interphase Mutual Inductance in Poly-Phase Inductive Power Transfer Systems," *IEEE Trans. Ind. Electron.*, vol. 56, no. 7, Jul. 2009

[6] L. Chen, G. R. Nagendra, J. T. Boys and G. A. Covic, "Double-coupled systems for IPT roadway applications," *IEEE Journal of Emerging and Selected Topics in Power Electronics,* doi: 10.1109/JESTPE.2014.2325943.

[7] S. Choi, J. Huh, W. Y. Lee, S. W. Lee, and C. T. Rim, "New crosssegmented power supply rails for roadway powered electric vehicles," *IEEE Trans. Power Electron.*, 2013, DOI: 10.1109/TPEL.2013.2247634

[8] G. Covic and J. T. Boys, "Modern trends in inductive power transfer for transportation applications," *IEEE Journal of Emerging and Selected Topics in Power Electronics*, vol. 1, no. 1 pp. 28 - 41, May 2013.

[9] T. Kudo, T. Toi, Y. Kaneko, S. Abe, "Contactless power transfer system suitable for low voltage and large current charging for EDLCs," *The 2014 Int. Power Electronics Conf.*, vol. , no. 20B1-2, pp. 1109-1114, 2014.

978-1-4799-6610-3/15/$31.00 ©2015 IEEE

[10] H. Irie and H. Yamana, “Immittance converters suitable for power electronics,” *Elect. Eng. Jpn*., vol. 124, no. 2, pp. 53–62, doi: 10.1002/(SICI)1520-6416(19980730)124:2<53::AID-EEJ7>3.0.CO;2-N

[11] K. E. Koh, T. C. Beh, T. Imura, and Y. Hori, “Impedance Matching and Power Division Using Impedance Inverter for Wireless Power Transfer via Magnetic Resonant Coupling,” *IEEE Trans. Ind. Appl.*, vol. 50, no. 3, pp. 2061-2070, Oct. 2013.

[12] C. Wang, G. A. Covic and O. H. Stielau, “Power transfer capability and bifurcation phenomena of loosely coupled inductive power transfer systems,” *IEEE Trans. Ind. Electron*, vol. 5, no. 1, Feb. 2004.

[13] K. V. Schuylenbergh and R. Puers, “Inductive powering: basic theory and application to biomedical systems,” Springer, 2009.

[14] M. Kato, “Wireless Power Transfer for Electric Vehicle via Magnetic Resonant Coupling,” Ph.D. dissertation, Dept. of Advanced Energy, the University of Tokyo, Kashiwa, Chiba, Japan, 2014

978-1-4799-6610-3/15/$31.00